SciMedCentral

Journal of Materials & Applied Science

Research Article

New Analytical Screening Method to Measure Chrysotile in Asbestos Containing Materials by Inductively Optical Emission and Mass Spectrometry Techniques Coupled Plasma

Andrea Chiappa[1], Carlo Iacovella[1], Daniele Raponi[1]*, Luigi Cassioli[1], Laura Allegrucci[1], Biagio Maria Bruni[2], Antonella Campopiano[3], Angelo Olori[3], Federica Angelosanto[3], Lorenzo Palumbo[2], Annapaola Cannizzaro[3] and Manuele Bernabei[1]

[1]*Aerospace Materials Technology Department, ITAF- Aerospace Testing Division, Aeroporto Militare De Bernardi, Rome, Italy*

[2]*Environments and Health Department, Italian National Institute of Health, Vaile Regina Elena, Rome, Italy*

[3]*Department of Medicine, Epidemiology, National Institute for Insurance against Accidents at Work, Workplace and Environmental Hygiene, Via Fontana Candida, Rome, Italy*

***Corresponding author**

Daniele Raponi, Aerospace Materials Technology Department, ITAF- Aerospace Testing Division, Aeroporto Militare De Bernardi, Rome, Italy

Submitted: 19 December 2023

Accepted: 16 January 2024

Published: 18 January 2024

ISSN: 2333-7133

Keywords

- Inductively Coupled Plasma Optical Emission and Mass Spectrometry Techniques (ICP-OES/MS)
- Chrysotile
- Linear Discriminant Analysis (LDA
- Quantitative Analysis
- Asbestos
- Fourier Transform Infrared Spectroscopy (FTIR)

Abstract

Although the World Health Organization has classified asbestos as a human carcinogen and many countries all around the world have banned or posed very strict restrictions to asbestos uses, its consumption is increasing worldwide as well as the incidence of asbestos-linked diseases. Current standard methods for asbestos analysis are very lengthy and costly and they suffer of poor detection limits, accuracy and precision, especially in the case of materials with low asbestos content.

Here we describe a new, fast, efficient and selective analytical screening method to perform a test for Chrysotile in suspected Asbestos Containing Materials (ACMs) grouped by commodity class and analyzed by Inductively Coupled Plasma Optical Emission and Mass Spectrometry Techniques (ICP-OES/MS). The outcomes were processed by means of the chemo metric approach of Linear Discriminant Analysis (LDA).

Here we demonstrate that this method permits to correctly classify the ACMs of specific commodity classes with the same performance than standard methods based on phase-contrast and electronic microscopy (PCM, FESEM) and Fourier Transform infrared spectroscopy (FTIR). Furthermore, this analytical approach offers a paramount advantage of an instrumental analytical technique with very high sensitivity and specificity, typical of trace element analysis techniques and suitable to automation process, definitely useful when extensive sampling plans are needed.

INTRODUCTION

Asbestos minerals worldwide-considered and regulated as human health threat are six species of hydrate silicate minerals with fibrous morphology: 1) Chrysotile, the most mined and commercialized, with ideal chemical formula $Mg_3Si_2O_5(OH)_4$, 2) Riebeckite amphibole, ideally $Na_2(Fe^{2+}{}_3Fe^{3+}{}_2)_{\Sigma=5}Si_8O_{22}(OH)_2$, usually referred as "crocidolite", 3) Granitite amphibole, ideally $Fe^{2+}{}_7Si_8O_{22}(OH)_2$, usually as "ammonites", 4) Anthophyllilte ideally $Mg_7Si_8O_{22}(OH)_2$, 5) Trifoliate amphibole, ideally $Ca_2Mg_5Si_8O_{22}(OH)_2$, 6) Actinolite amphibole, ideally $Ca_2Fe^{2+}{}_5Si_8O_{22}(OH)_2$.

Asbestos materials were widely used in the past to produce almost an uncountable number of reinforced type materials both for building and technological purposes (e.g. floor tiles, wall boards, thermal gaskets, asbestos cement, glues, etc.) [1]. Although the asbestos carcinogenicity risk assessment was evaluated by [2] and most of the countries all around the world banned or posed very strict restrictions to asbestos uses [3], asbestos correlated diseases are still a concern [4] because of the increasing asbestos consumption in the so called B.R.I.C.S. Area [5] and its natural presence up to soil's surface [6,7].

Consequently, the ability to perform fast and effective sampling and monitoring campaigns at lowest level of detection is of paramount importance to properly manage the asbestos risks. Current standard methods for qualitative and quantitative analysis of asbestos in asbestos containing materials are based on Microscopy [8,9] and Spectroscopy [10-14] they are generally

used for a restricted type of materials, they need a specific sample treatment to obtain low-level detection limits [15,16] and an experienced operator with very specific technical skills is required. Furthermore, microscopic methods suffer of poor sample representativeness while spectroscopic and diffract metric techniques suffer of poor detection limits, about 1%, accuracy and precision. Since they are very lengthy and costly, the samplings of suspected asbestos containing materials are often reduced to a limited number of samples.

For all of these issues and considering the REACH constraints about monitoring asbestos containing goods in the UE [17], academic and industrial researchers are constantly engaged in developing innovative analytical methods to improve accuracy, sensitivity, representativeness and cost-effectiveness [18].

The aim of this work is the validation of a rapid analytical screening method able to intercept Chrysotile containing materials and estimate the concentration of Chrysotile, certifying when possible the absence of Chrysotile in asbestos-free materials below 1% w/w, where standard methods have the greatest uncertainty, due essentially to their poor sensitivity.

The proposed method is based on mineralization of samples in acid environments [19-24] followed by elemental analysis via Inductively Coupled Plasma equipped with either optical emission spectroscopy (ICP-OES) or Mass Spectrometry (ICP-MS). Although the asbestos chemical composition has been already used mainly to study health hazards [25,26], interest in potential analytic purposes has been recently increasing [27].

In this study three common commodity classes of Chrysotile containing materials (vinyl floor, gaskets and concrete materials) with typical Chrysotile content between 5-50% w/w were taken into account [28-31]. Data were processed by Linear Discriminant Analysis (LDA) [32] in order to intercept Chrysotile in the samples as effectively as the standard test methods. Similar statistical elaborations have been recently adopted to detect and classify asbestos fibers [33,34].

The treatment of the samples is very fast and simple; it requires a larger amount of the sample than standard techniques, ensuring a proper representativeness of the original materials. The leaching of elements like Fe and Mg reduces the danger of any asbestos and health risks for the operators as well [25]. The analysis can be automatized (automated) in case of large number of samples.

EXPERIMENTAL

Materials and Samples

Reference Materials (Table S4) were prepared using polytetrafluoroethylene powder (mean particle size 20 µm - ACROS), Chrysotile standard NIOSH/IITRI CH-29 (Impurities 1-2% Steel fragments, 1-2% carbonate minerals, 1% quartz, 1% iron oxides, < 0.5% massive serpentine), 2-propanol RPE Grade (Carlo Erba), Ethyl 2-Cyanoacrylate (Sigma Aldrich). For

Table S4: List of Reference Materials for Quality Control in analytical sequences and Chrysotile concentrations, expressed in mass percent (w/w)%.

	Matrix	Chrysotile, (w/w)%
Ref. Mat. 1	Vinyl floor tile	2.90 ± 0.01
Ref. Mat. 2	Ethyl 2-cyanoacrylate	0.85 ± 0.01
Ref. Mat. 3	PTFE pellets	0.96 ± 0.01
Ref. Mat. 4	PTFE pellets	0.08 ± 0.01
RTI std 09	RTI International vinyl standards	2 - 6
RTI Std 10	RTI International organic matrix standard	3 - 6

mineralization and ICP analysis were used Ultrapure Water (18.2 MΩ a 25°C), HNO3 68% RPE Grade, HCl 37% RPE Grade, KBr RPE Grade and mono-element standard solution (Co, Ni, Fe, Mn, Cr, Mg) 1000 mg/L.

Training set consisted of fifty samples of suspect asbestos containing materials (twenty-five vinyl floors, fifteen gaskets and ten concrete). Thirteen samples of suspected Chrysotile materials, coming from 2020-2022 Laboratories program qualification organized by Italian Ministry of Health were included in the Control set.

Methods and Instruments

Standard techniques analysis: The microstructural examination of the samples was performed by field emission scanning electron microscopy (FE-SEM, Zeiss, Merlin), operated at an accelerating voltage of 15 kV, a probe current of 150 PA, a working distance of 8.5 mm and zero degrees tilt. The detector used was a secondary electron detector. An energy dispersive spectrometer (EDS, Oxford Instrument INCA) coupled with FE-SEM allowed a compositional analysis of the sample.

Fourier Transform Infrared spectra were obtained using either in diffuse reflectance (FTIR, Spectrum One, Perkin Elmer) or in transmission to analyze ultrapure KBr pellets [35] (Spectrum™ 3 FTIR). The operative parameters of the instruments were acquisition range 4000 - 400 cm^{-1}, resolution 4 cm^{-1} and 32 scans. In transmission mode the optical compartment of the instrument was flushed with nitrogen before starting sample analysis. Before each scan, the sample compartment has been saturated with the same gas for about ten minutes to clear the air. All samples were weighted by a Sartorius scale (MC1, capacity 210 g, precision 0.01 mg, SARTORIUS AG) equipped with a device to neutralize electrostatic charges. The weighted quantities were in the range 50 µg - 2 mg. Each sample was mixed with about 250 mg of pure KBr previously dried in the 300 - 400°C range in a muffle furnace (Gefran 400) for 3-5 days. The background can be measured with either an empty pellet holder inserted into the sample chamber or with a pellet holder with an ultrapure KBr pellet, which contains no sample.

X-ray Diffraction Analysis were performed with a Bruker D8 Da Vinci Advanced Diffract meter in this configuration: Source: Tube Cu Kα 1.5406 Å, Scan range 5°-50°, Step size 0.010°, Time for step 1s, Detector Lynxeye-2 Mod 1D. Samples were prepared by grinding in a mill, dispersion in aqueous solution and deposition on a silver filter of an amount between 100 - 300 µg.

Inductively Coupled Plasma Optical Emission and Mass Spectrometry Techniques (ICP-OES/MS): An amount of 10.0 ± 1.0 mg standard asbestos fibers was introduced into a 75 mL digestion vessels, adding 1.0 mL of ultrapure water, then 5.0 mL of HNO3 68% RPE and 4.0 mL of HCl 37% RPE were introduced. Digestion process was carried out by CEM Corporation MARS 5 Digestion Microwave System. Digestion set-up for 12 vessels: 10 min at 800 W + 10 min at 1600 W. Vessel was cooled to room temperature and the extract diluted with UP water into a 50.0 mL flask followed by a centrifugation step to remove solid precipitate; finally supernatant was analyzed. The same procedure was carried out to process asbestos containing materials grinding at least 300 mg of the sample in an agate mortar for 2 - 5 minutes to achieve approximately 200 µm of granulometry, eventually 100.0 ± 10.0 mg of the sample were used. Digestion solutions were analyzed either in ICP-OES (Perkin Elmer OPTIMA 2100DV) or analyzed in ICP-MS (Agilent 7500cx); regarding to ICP-OES no dilution is generally necessary if values fall in calibration linear range instead in ICP-MS dilution between 1:10 and 1:20 in water UP is generally necessary to reduce isobaric interference due to high concentrations of chloride ions; Sc and Ho can be used as internal standard. The analytical sequence included a Method Blank and a Laboratory Control Sample. Analytical conditions are reported in (Table S5,S6).

Quantitative estimate of Chrysotile (ChryEQ)

The quantitative estimate of Chrysotile content (ChryEQ) was calculated converting the elements' concentration in Chrysotile's mass percentage, using a statistically representative composition reported in (Table S7).

Table S5: ICP-OES instrumental conditions.

Parameters	Operative conditions
Radiofrequency power	1400 W
Argon cooling flow	15 L/min
Argon flow	0.7 L/min
Auxiliary argon flow	0.2 L/min
Injector diameter	2 mm
Internal standard	Sc
Analytes (wavelength nm)	Mg (280.271/ LOD 0.001 mg/L), Cr (267.716 / / LOD 0.01 mg/L), Mn (257.610 / LOD 0.002 mg/L), Fe (238.204 / LOD 0.05 mg/L), Co (228.616 / LOD 0.007 mg/L), Ni (231.604 / LOD 0.015 mg/L)

Table S6: ICP-MS instrumental conditions.

Parameters	Operative conditions
Radiofrequency power	1500 W
Plasma Argon flow	15 L/min
Carrier gas Argon flow	0.9 L/min
Auxiliary argon flow	0.9 L/min
Makeup gas Argon flow	0.21 L/min
He gas flow (collision cell)	4.7 mL/min
Sampling speed	0.10 rps
Internal standard	Sc, Ho
Analytes (m/z – tune mode - LOD)	Mg (24 – He – LOD 22.8 ng/L), Cr (53 – He - LOD 3.20 µg/L), Mn (55 – nogas - LOD 0.21 ng/L), Fe (56 – He - LOD 30.0 ng/L), Co (59 – He - LOD 0.002 ng/L), Ni (60 – no gas - LOD 0.78 ng/L)

Table S7: Statistically representative Chrysotile's composition (expressed in mg/kg). Median (Central trend), Upper Limit Confidence Interval 95% (Upper Limit), Lower Limit Confidence Interval 95% (Lower limit).

	Upper Limit CI95% (mg/kg)	Median (mg/kg)	Lower Limit CI95% (mg/kg)
Mg	246300	243000	238800
Fe	25110	18000	14000
Cr	780	490	380
Mn	600	480	444
Ni	1360	830	802
Co	60	53	50

The values were defined by a systematic review of studies in the literature [20,23,36-39]. The central trend is expressed by the median, which is preferable when the distribution of the data is asymmetrical due to outliers or indeterminate values, while the dispersion of data is expressed in terms of Confidence Interval of 95% [40-43].

Linear Discriminant Analysis (LDA)

LDA is a statistical tool used for classification, dimension reduction and data visualization. The classification algorithm is developed according to a series of objects with a known classification (training set). LDA was performed for each commodity class with Statistical 10 software using 7 variables, 6 of which refer to the chemical composition and 1 to the estimate of Chrysotile. A priori probability was set the same for each class. The LDA algorithm was evaluated by Will's lambda test and p-value and finally it was applied to Control Set. LDA results were matched with FE-SEM and FTIR results [44-46].

RESULTS AND DISCUSSION

Method's Repeatability and Recovery Efficiency

Regarding to performance of the method, data are reported in (Table 1). The digestion efficiency of leaching process was carried out on 10.0 ± 1.0 mg of standard Chrysotile (NIOSH CH-29) by measuring concentration of six target elements. Ten replicates were carried out in order to evaluate the digestion repeatability. Relative Standard Deviation percentage (RSD %) varies between 4.9 - 12.9%. The value for Mg, the main element, is 4.9% while the values for the other target elements are in the 5.1% - 7.7% range. Only Cobalt, which was found in trace amounts in Chrysotile, showed a 12.9% RSD%. This evidence demonstrates that leaching process of Chrysotile has good repeatability.

In order to evaluate the extraction efficiency of whole analytical process (grinding, digestion and ICP-OES/MS analysis), the recovery (%) was determined on four Reference Materials. The experimental values for [1,2] are very good (inside 92-103% for Mg and 85-120% for other elements). Cobalt concentration is lower than ICP-OES detection limits. Values for Reference Materials 3 and 4 are generally acceptable, even though many of the analytical targets are below the ICP-OES detection limits, suggesting the need of ICP-MS when ultra-trace concentrations are expected.

Finally, Chrysotile content (ChryEQ) in six reference materials was evaluated converting elemental composition data in mass

Table 1: Method's Performance (Repeatability, Recovery %, Chrysotile estimate) evaluated on Reference Materials.

	Reference Materials/lement	Chrysotile NIOSH CH-29	Ref. Mat. 1	Ref. Mat. 2	Ref. Mat. 3	Ref. Mat. 4	RTI Std 09	RTI Std 10
Method's Repeatability (RSD%, n=10)	Co	12.9%	-	-	-	-	-	-
	Ni	5.7%	-	-	-	-	-	-
	Fe	7.7%	-	-	-	-	-	-
	Mn	5.3%	-	-	-	-	-	-
	Cr	5.1%	-	-	-	-	-	-
	Mg	4.9%	-	-	-	-	-	-
Method's Recovery (% w/w)	Co	-	< LOD	< LOD	< LOD	< LOD	-	-
	Ni	-	100%	108%	68.6%	< LOD	-	-
	Fe	-	88.0%	120%	66.5%	102%	-	-
	Mn	-	96.4%	106%	74.7%	< LOD	-	-
	Cr	-	95.9%	84.5%	89.6%	< LOD	-	-
	Mg	-	92.4%	103%	119%	68.6%	-	-
Chrysotile Estimate (% w/w)	$CriEQ_{Co}$	-	< LOD	< LOD	< LOD	< LOD	4.78	4.74
	$CriEQ_{Ni}$	-	5.09	1.74	1.14	< LOD	13.4	16.9
	$CriEQ_{Fe}$	-	3.94	1.11	0.67	0.23	16.7	20.6
	$CriEQ_{Mn}$	-	15.29	0.97	0.74	< LOD	30.8	12.6
	$CriEQ_{Cr}$	-	8.33	2.84	2.28	< LOD	17.8	5.70
	$CriEQ_{Mg}$	-	2.96	0.90	1.10	0.06	11.0	10.6
	CriEQ	-	2.96	0.90	0.67	0.06	4.78	4.74
	Declared value	-	2.90	0.85	0.96	0.08	2 - 6	3 - 6
	Δ	-	+ 2.1%	+ 9.7%	- 30.2%	- 25.0%	inside range	inside range

percentage of Chrysotile using the above mentioned statistically representative Chrysotile's chemical composition, without any further analytical effort. ChryEQi values for each element (i= Mg, Fe, Mn, Cr, Co, Ni) are reported in (Table 1), while upper and lower bounds of confidence interval of 95% are plotted in (Figure 1). As expected, the ChryEQMg values are the most accurate due to the low variability of this constitutive element in the Chrysotile. Other elements, as not constitutive, suffer of a higher variability and so the corresponding ChryEQi as well. Regarding to accuracy, ChryEQi values are expected as an overestimation of the real Chrysotile content in the Reference Materials due to the fact that in the calculation are considered the total elements' concentrations, including the matrix's contribution. In order to minimize the matrix interference, minimum among the ChryEQi values for each sample is considered to be the best estimate of Chrysotile in the material. ChryEQi values for [1,2] are in good accordance with declared values, respectively +2.1% and +9.7%. Values for [3,4] are generally lower down to about 30% than declared values, essentially due to the extremely high resistance to acidic digestion of polytetrafluoroethylene used as matrix. Values for RTI STD 09 and STD 10 fall perfectly in the range declared on the certificates of materials. Estimation of Chrysotile by ChryEQMg is in general the most accurate [1-4] but regarding to RTI Standards 09 and 10, in which the known Mg matrix interference is due to the presence of Dolomite CA Mg $(CO_3)_2$, the least interfered element is Co, whose concentration was determined by ICP-MS as it was lower than the ICP-OES detection limits. This highlights the need of more sensitive detection to correctly quantify secondary targets and then to mitigate the possible matrix interference in Mg content.

Recognition of Chrysotile Containing Materials by LDA and Estimate of Chrysotile Content

The method proposed is applicable to commodity classes that are included in training set, which are in this case vinyl floor tiles, gaskets and concrete materials. Training and Control set samples had been previously classified as asbestos positive/negative by standard techniques (Figure S1) and then analyzed by ICP-OES/MS; the elemental analysis results and the estimates of Chrysotile are reported in (Table 2). Single ChryEQi are instead reported in (Table S8). For what concerns Training set, elements like Co, Ni and Cr are critical because of the instrumental sensitivity. The concentration of these elements in the asbestos-free samples is often lower than the ICP-OES detection limits while for Chrysotile containing samples all the elements are above them. This does not limit the capability of Linear Discriminant Analysis to correctly intercept Chrysotile containing materials for the considered commodity classes (typical Chrysotile content from 5% to 50%), but in case of commodity classes with typical Chrysotile content below 5%, the ICP-MS should be used. Regarding to Control set, the use of ICP-MS instead of ICP-OES allowed, in fact, to quantify all the elements also in asbestos-free samples and to identify typical concentration patterns.

The plot in (Figure 2) shows training set samples in descending order of Chrysotile estimate with a perfect separation between asbestos free (white columns) and Chrysotile containing materials (dashed columns). Moreover, all values are in accordance with the typical formulations of these commodity products (Chrysotile between 5 and 50 % w/w), except for sample G-08, which is just inside the area of positivity even if negative (5.3 % w/w).

Differences in ChryEQ between asbestos free and Chrysotile containing materials are evident (Figure 3), especially for vinyl floors and gaskets. The box-whiskers plots report the statistics

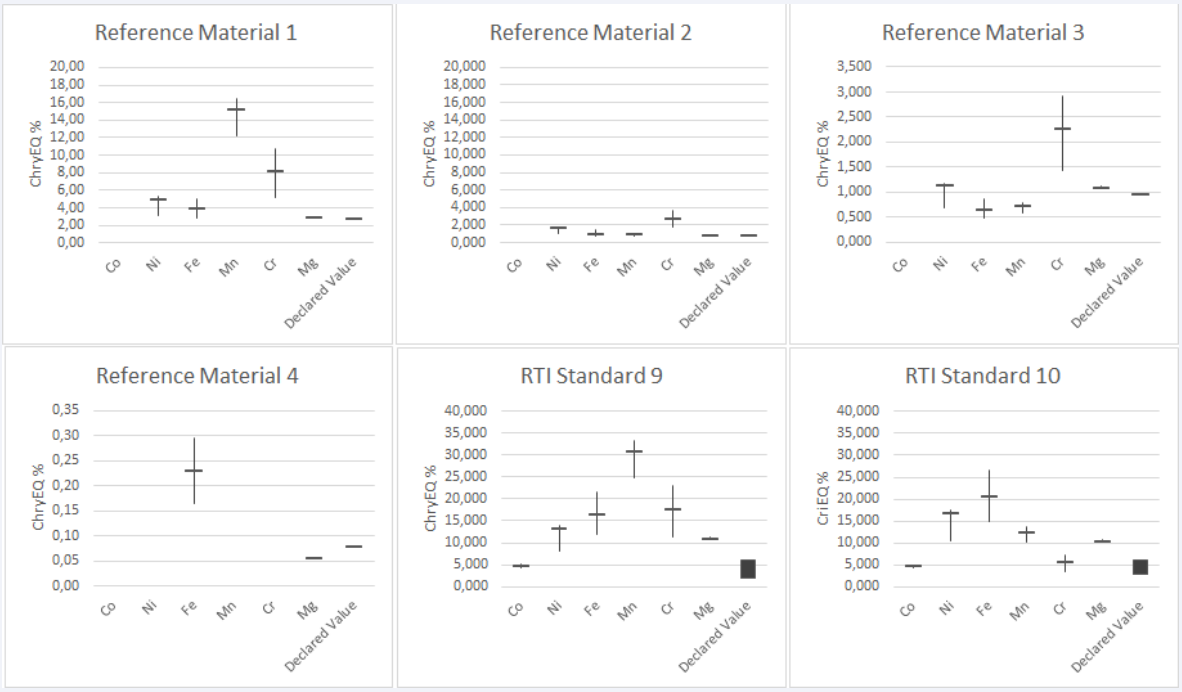

Figure 1 ChryEQ for reference materials (expressed in % w/w) referred to median value, Upper Limit of CI95% and Lower Limit of CI95%.

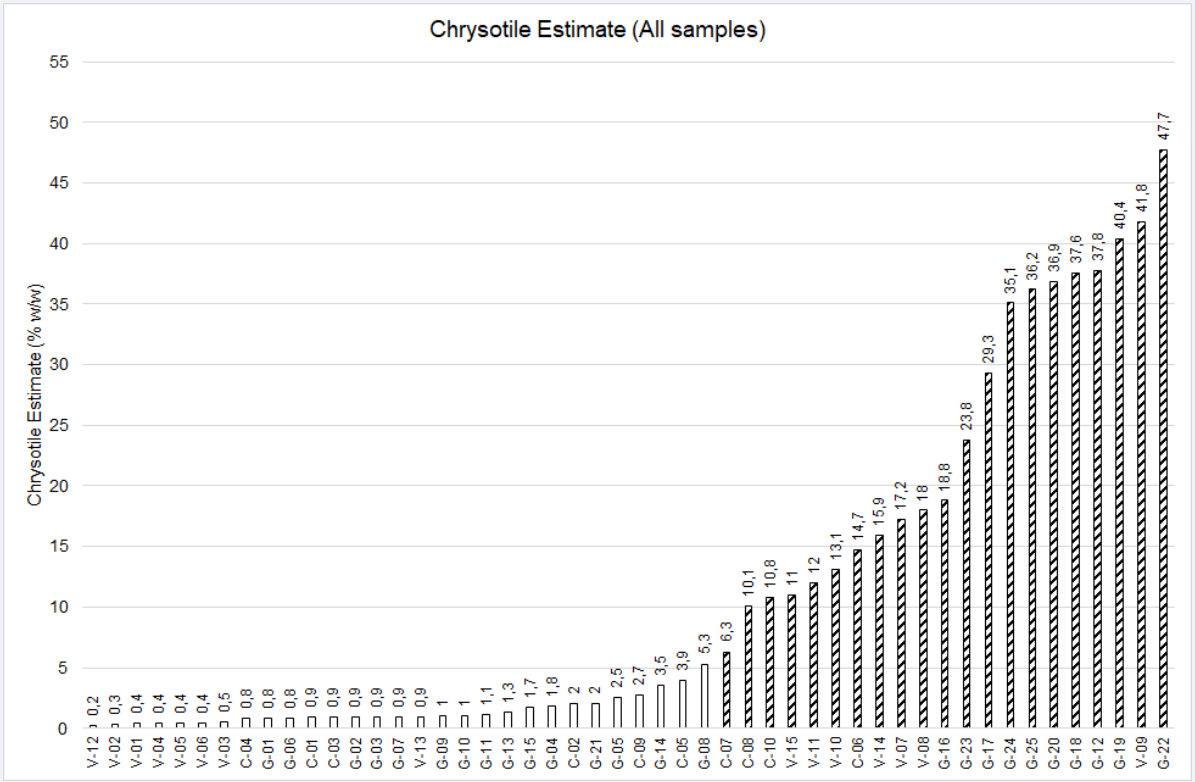

Figure 2 ChryEQ for all training set samples: Chrysotile containing samples (dashed columns) and asbestos-free samples (white columns) to Chrysotile. Typical Chrysotile concentration in considered commodity classes (5-50% w/w).

Technical Sheet Sample Vinyl floor 10 : Vinyl tile blue/gray.

naked eye image of sample

PCM. Chrysotile Fiber in 1.55 stunning liquid-0°polarized light

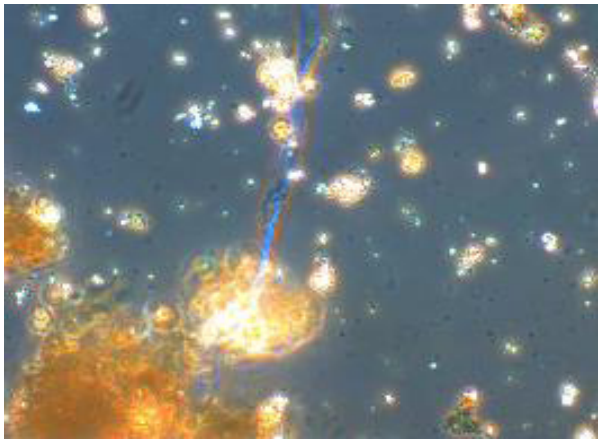

SEM image of fibers in the sample

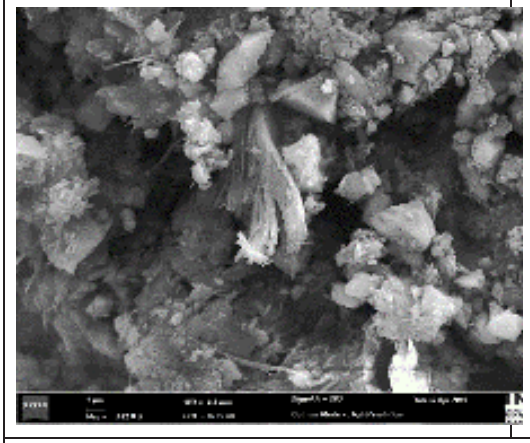

SEM-EDS Spectrum for Chrysotile fibers identification

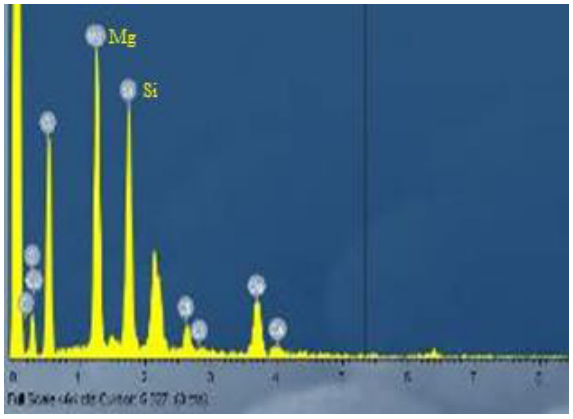

FTIR Spectrum, (Absorbance) with diagnostic peaks for Chrysotile reported.

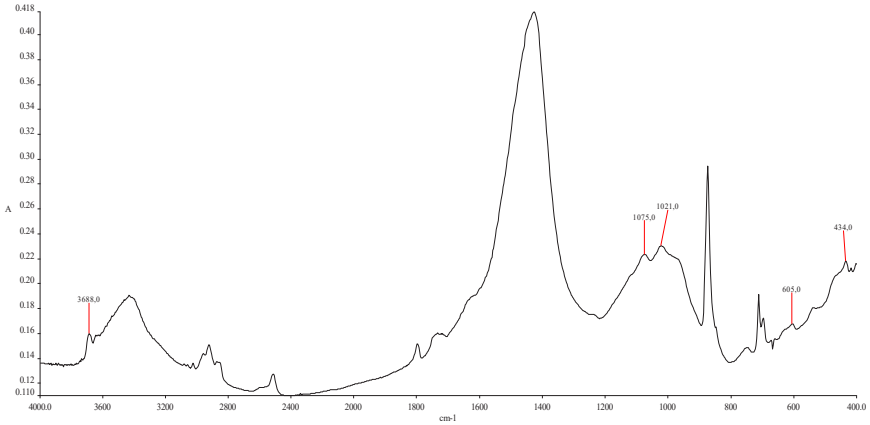

Quantification of Chrysotile via mineralization and ICP OES analysis

Sample	Mg (mg kg $^{-1}$)	Cr (mg kg $^{-1}$)	Mn (mg kg $^{-1}$)	Fe (mg kg $^{-1}$)	Ni (mg kg $^{-1}$)	Co (mg kg $^{-1}$)
Vinyl floor 10	3.19E+04	1.69E+02	2.81E+02	1.43E+04	1.97E+02	1.47E+01

ChryEq = 13.0 -13.4% (UCL – LCL%, coherent with typical asbestos formulation for Vinyl Floor Chrysotile tiles)

Figure S1 Sample technical sheet – example for Sample Vinyl floor 10.

Table 2: Training Set and Control Set samples: samples' codes, classification by standard techniques and LDA, elemental composition expressed in mg/kg (values in bracket are < LOD method via ICP OES), Chrysotile's estimate (ChryEQ).

		Std	LDA	Target element's sample concentration as mg kg^{-1}						ChryEQ
	Code	Classification	Classification	Co	Ni	Fe	Mn	Cr	Mg	(% w/w)
	C-01	Neg	-	4.71E + 00	7.07E + 00	1.11E + 04	4.13E + 02	1.51E + 01	2.90E + 03	0.9
TRAINING SET	C-02	Neg	-	< (3.44E + 00)	1.67E + 01	9.72E + 03	5.14E + 02	1.72E + 01	5.63E + 03	2.0
	C-03	Neg	-	< (3.49E + 00)	< (7.47E + 00)	1.10E + 04	3.25E + 02	8.97E + 00	4.83E + 03	0.9
	C-04	Neg	-	< (3.14E + 00)	< (6.72E + 00)	5.36E + 03	1.98E + 02	< (4.48E + 00)	2.30E + 03	0.8
	C-05	Neg	-	5.70E + 00	3.25E + 01	9.45E + 03	3.18E + 02	3.42E + 01	1.47E + 04	3.9
	C-06	Pos	-	2.41E + 01	2.41E + 02	2.10E + 04	6.78E + 02	1.33E + 02	3.56E + 04	14.7
	C-07	Pos	-	3.48E + 00	5.23E + 01	7.29E + 03	8.23E + 01	2.07E + 02	2.89E + 04	6.3
	C-08	Pos	-	1.41E + 01	2.48E + 02	1.58E + 04	2.81E + 02	1.00E + 02	2.45E + 04	10.1
	C-09	Neg	-	< (5.09E + 00)	2.26E + 01	6.46E + 03	1.92E + 02	1.98E + 01	6.96E + 03	2.7
	C-10	Pos	-	1.25E + 01	1.85E + 02	1.45E + 04	2.94E + 02	1.12E + 02	2.62E + 04	10.8
	G-01	Neg	-	< (3.46E + 00)	< (7.03E + 00)	1.66E + 02	3.95E + 00	1.28E + 01	5.86E + 03	0.8
	G-02	Neg	-	< (3.34E + 00)	< (7.14E + 00)	2.51E + 02	1.19E + 01	8.10E + 00	6.93E + 04	0.9
	G-03	Neg	-	< (3.54E + 00)	1.16E + 01	1.97E + 03	4.95E + 01	4.55E + 00	8.76E + 03	0.9
	G-04	Neg	-	< (3.61E + 00)	3.86E + 01	1.76E + 05	6.90E + 02	3.97E + 01	4.32E + 03	1.8
	G-05	Neg	-	6.86E + 01	4.65E + 03	3.26E + 04	6.81E + 02	8.17E + 03	6.19E + 03	2.5
	G-06	Neg	-	< (3.03E + 00)	< (6.50E + 00)	3.17E + 03	3.21E + 01	4.81E + 01	2.17E + 03	0.8
	G-07	Neg	-	< (3.42E + 00)	< (7.33E + 00)	1.42E + 03	5.43E + 01	5.77E + 01	4.51E + 03	0.9
	G-08	Neg	-	4.44E + 01	1.93E + 03	1.40E + 04	2.74E + 02	3.31E + 03	1.30E + 04	5.3
	G-09	Neg	-	< (3.29E + 00)	8.47E + 00	5.89E + 03	2.79E + 02	5.03E + 01	3.45E + 03	1.0
	G-10	Neg	-	< (3.17E + 00)	8.62E + 00	5.71E + 03	2.67E + 02	5.22E + 01	3.39E + 03	1.0
	G-11	Neg	-	< (3.31E + 00)	9.44E + 00	6.66E + 03	2.84E + 02	5.29E + 01	3.57E + 03	1.1
	G-12	Pos	-	4.87E + 01	3.79E + 04	1.08E + 04	2.39E + 02	7.97E + 03	9.19E + 04	37.8
	G-13	Neg	-	< (2.91E + 00)	1.45E + 01	9.08E + 03	2.96E + 02	6.54E + 00	5.79E + 03	1.3
	G-14	Neg	-	9.24E + 00	2.93E + 01	1.33E + 04	5.40E + 02	1.66E + 02	1.79E + 04	3.5
	G-15	Neg	-	< (3.41E + 00)	1.41E + 01	9.93E + 03	2.33E + 02	2.49E + 02	7.34E + 03	1.7
	G-16	Pos	-	1.46E + 01	4.46E + 02	3.38E + 03	1.13E + 02	1.95E + 02	7.58E + 04	18.8
	G-17	Pos	-	2.32E + 01	7.04E + 02	5.28E + 03	1.69E + 02	3.19E + 02	1.23E + 05	29.3
	G-18	Pos	-	3.04E + 01	8.12E + 02	6.76E + 03	2.03E + 02	4.13E + 02	1.31E + 05	37.6
	G-19	Pos	-	3.13E + 01	8.28E + 02	7.27E + 03	2.19E + 02	4.60E + 02	1.36E + 05	40.4
	G-20	Pos	-	3.43E + 01	9.05E+02	6.65E+03	2.06E+02	4.18E+02	1.29E+05	36.9
	G-21	Neg	-	< (3.53E + 00)	9.33E + 01	4.20E + 02	1.36E + 01	4.23E + 01	4.92E + 03	2.0
	G-22	Pos	-	3.24E + 01	5.25E + 02	1.21E + 05	7.45E + 02	2.41E + 02	1.16E + 05	47.7
	G-23	Pos	-	1.93E + 01	5.97E + 02	4.34E + 03	1.40E + 02	2.47E + 02	5.79E + 04	23.8
	G-24	Pos	-	2.83E + 01	7.37E + 02	6.31E +03	1.95E + 02	4.01E + 02	1.22E + 05	35.1
	G-25	Pos	-	2.84E + 01	7.78E + 02	6.51E + 03	1.83E + 02	3.78E + 02	1.22E + 05	36.2
	V-01	Neg	-	< (3.54E + 00)	2.84E + 01	1.15E + 02	1.22E + 01	< (2.02E + 00)	2.59E + 03	0.4
	V-02	Neg	-	< (3.58E + 00)	< (7.68E + 00)	1.84E + 02	5.73E + 01	< (4.09E + 00)	7.70E + 02	0.3
	V-03	Neg	-	< (3.58E + 00)	< (7.68E + 00)	1.76E + 02	1.76E + 01	< (2.56E + 00)	4.71E + 03	0.5
	V-04	Neg	-	< (3.58E + 00)	< (7.68E + 00)	1.55E + 02	6.15E + 01	< (5.12E + 00)	9.39E + 02	0.4
	V-05	Neg	-	< (3.21E + 00)	< (6.88E + 00)	1.79E + 03	2.33E + 02	< (1.84E + 00)	5.00E + 04	0.4
	V-06	Neg	-	< (3.30E + 00)	7.08E + 00	1.90E + 02	2.97E + 01	< (2.83E + 00)	9.14E + 02	0.4
	V-07	Pos	-	1.44E + 01	3.30E + 02	6.92E + 03	8.27E + 01	2.40E + 02	4.67E + 04	17.2
	V-08	Pos	-	1.29E + 01	2.89E + 02	8.68E + 03	1.06E + 02	1.90E + 02	4.38E + 04	18.0
	V-09	Pos	-	6.18E + 01	1.24E + 03	2.50E + 04	4.87E + 02	6.81E + 02	1.02E + 05	41.8
	V-10	Pos	-	1.47E + 01	1.97E + 02	1.43E + 04	2.81E + 02	1.69E + 02	3.19E + 04	13.1
	V-11	Pos	-	1.03E + 01	2.34E + 02	5.75E + 03	1.65E + 02	1.92E + 02	2.93E + 04	12.0
	V-12	Neg	-	< (3.02E + 00)	< (6.48E + 00)	2.13E + 03	5.88E + 01	1.43E + 01	4.45E + 02	0.2
	V-13	Neg	-	< (3.52E + 00)	< (7.55E + 00)	4.35E + 03	2.47E + 01	6.01E + 02	2.98E + 03	0.9
	V-14	Pos	-	1.43E + 01	3.10E + 02	7.35E + 03	7.64E + 01	7.70E + 02	5.02E + 04	15.9
	V-15	Pos	-	5.83E + 00	1.52E + 02	1.37E + 04	1.28E + 02	1.81E + 02	2.67E + 04	11.0
CONTROL SET	C-11	Pos	Pos	9.35E + 00	1.35E + 02	1.61E + 04	2.99E + 02	8.71E + 01	2.56E + 04	10.5
	C-12	Pos	Pos	4.35E + 01	1.19E + 03	1.50E + 04	3.71E + 02	5.58E + 02	2.06E + 05	77.4
	C-13	Pos	Pos	9.90E + 00	1.44E + 02	1.71E + 04	3.05E + 02	1.32E + 02	2.50E + 04	10.3
	C-14	Neg	Neg	3.68E + 00	2.72E + 01	6.10E + 03	2.26E + 02	3.98E + 01	6.47E + 03	2.7
	C-15	Neg	Neg	4.06E + 00	3.03E + 01	6.86E + 03	2.47E + 02	4.88E + 01	7.32E + 03	3.0
	G-26	Pos	Pos	3.99E + 01	1.15E + 03	1.48E + 04	2.74E + 02	4.97E + 02	1.84E + 05	57.1
	V-16	Neg	Neg	5.85E - 01	3.07E + 00	7.95E + 02	5.85E + 00	4.09E + 01	1.91E + 03	0.4
	V-17	Pos	Pos	4.56E + 01	8.00E + 02	2.61E + 04	1.04E + 03	7.80E + 02	1.17E + 05	48.0
	V-18	Pos	Pos	1.32E + 01	2.70E + 02	6.68E + 03	1.20E + 02	2.61E + 02	5.21E + 04	21.4
	V-19	Pos	Pos	1.33E + 01	2.60E + 02	5.27E + 03	1.03E + 02	6.39E + 02	4.58E + 04	18.8
	V-20	Neg	Neg	7.43E - 01	4.02E + 00	5.91E + 02	7.34E + 00	5.81E + 00	1.21E + 03	0.5
	V-21	Pos	Pos	1.20E + 01	2.42E + 02	6.59E + 03	8.83E + 01	2.34E + 02	4.66E + 04	18.4
	V-22	Neg	Neg	7.07E + 00	1.45E + 02	5.52E + 03	1.60E + 02	7.43E + 01	1.06E + 04	4.4

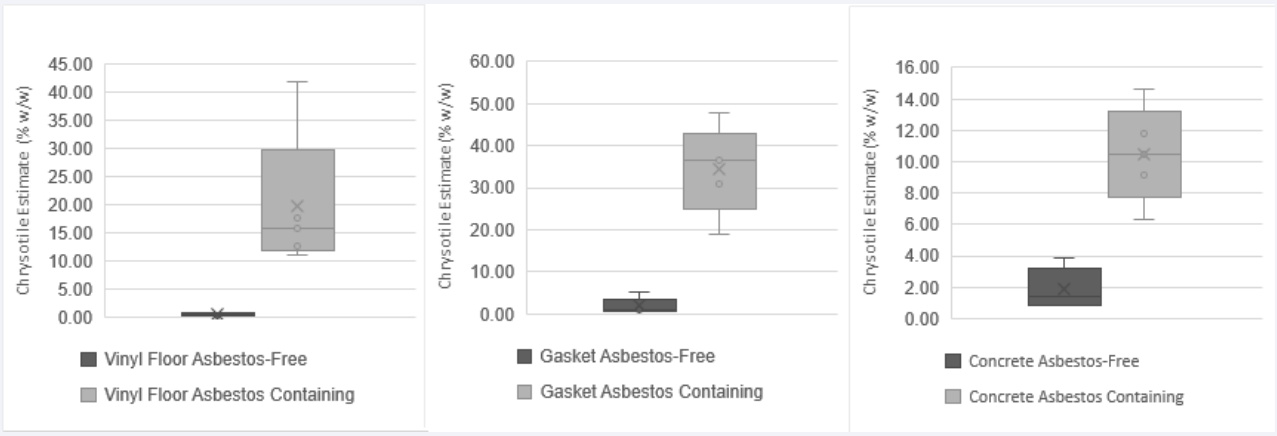

Figure 3 Statistics of the ChryEQ in training set bulk samples. Box-whiskers plot reports minimum, maximum, 25th and 75th percentiles and median value.

Table 3: Linear Discriminant Analysis summary: Wilks' Lamba and *p*-values.

Comm. Classes	Wilks' Lambda	*P*-values						
		Co	Ni	Fe	Mn	Cr	Mg	ChryEQ
Concrete	0.00379	0.3509	0.3198	0.3255	0.3668	0.0376	0.1488	0.2357
Gasket	0.08082	0.3825	0.3757	0.9539	0.3511	0.3737	0.6985	0.0083
Vinyl Floor	0.0244	0.0341	0.9988	0.5284	0.0572	0.2268	0.0899	0.0004

of the ChryEQ in training set samples (minimum, maximum, 25th and 75th percentiles and median value) of asbestos-free materials and Chrysotile containing materials respectively for concretes, gaskets, and vinyl floors. For all commodity types, the statistic scores for asbestos containing materials are significantly higher than for asbestos-free samples.

Finally, linear discriminant analysis was applied to analytical data for each commodity class using data reported in [Table 2] in order to recognize asbestos containing materials. The algorithms obtained very small Wilks' Lambda values for all commodity classes, which indicate a good discriminating power of the model (Table 3). Furthermore, considering the single variables, ChryEQ confirms to have a good discriminant power (small p-value) but, at the same time, also other elements, like for instance Cobalt in vinyl floor and Chromium in concrete, significantly contribute to discriminate positive and negative samples. As a result, Control set samples were all correctly classified by LDA according to traditional techniques results (Table 2).

CONCLUSION

The use of elemental analysis coupled with linear discriminant analysis was effective to classify samples like positive or negative and give a quantitative estimation of a theoretical maximum allowable Chrysotile in a set of 50 samples, verified by traditional techniques.

Asbestos-free samples are often characterized by a not detectable level for at least one target element (Cobalt, Nickel or Chromium) in ICP-OES. This approach seems very effective for vinyl floor samples to verify asbestos-free condition down to a 0.2% and, theoretically, down to 0.0002 % w/w, considering the sensitivity of applied analytical techniques, when traditional methods suffer poor quantification limit, around to 1% w/w.

This method can be a very useful pre-screening method and co-investigation technique for ACMs analysis, especially in combination with FTIR and XRD analysis for both organic and inorganic matrices. It can be automated as a screening process for large number of samples, providing a dramatic reduction of samples to analyze with the current standard methods.

For asbestos-free debate samples, it could be valid tool to refine as much as needed the allowable theoretical maximum Chrysotile content in the sample. Extension of this analytical approach to airborne samples and amphiboles could increase complexity but appears possible.

ACKNOWLEDGMENT

Authors wish to thank Dr. Gargaro Giuseppe and Dr. November Giuseppina of INAIL for technical support to SEM microscopy analysis.

Conflict of Interest

The authors declare no known of competing financial interests or personal relationships that could have influence in the work reported in this paper.

Table S8: ChryEQ$_t$ calculated respectevely by ICP OES for Training Set samples and by ICP MS for Control Set. Corresponding classification by standard techniques and Linear Discriminant Analisys. The values in brackets are calculated on the basis of the ICP OES detection limits.

	#	Commodity	CriEQ$_{Co}$ (% w/w)	CriEQ$_{Ni}$ (% w/w)	CriEQ$_{Fe}$ (% w/w)	CriEQ$_{Mn}$ (% w/w)	CriEQ$_{Cr}$ (% w/w)	CriEQ$_{Mg}$ (% w/w)	**CriEQ (% w/w)**
TRAINING SET	C-01	Concrete	8.9	0.9	61.7	86.0	3.1	1.2	**0.9**
	C-02	Concrete	(6.5)	2.0	54.0	107.1	3.5	2.3	**2.0**
	C-03	Concrete	(6.6)	(0.9)	61.1	67.7	1.8	2.0	**0.9**
	C-04	Concrete	(5.9)	(0.8)	29.8	41.3	(0.9)	0.9	**0.8**
	C-05	Concrete	10.8	3.9	52.5	66.3	7.0	6.0	**3.9**
	C-06	Concrete	45.5	29.0	116.7	141.3	27.1	14.7	**14.7**
	C-07	Concrete	6.6	6.3	40.5	17.1	42.2	11.9	**6.3**
	C-08	Concrete	26.6	29.9	87.8	58.5	20.4	10.1	**10.1**
	C-09	Concrete	(9.6)	2.7	35.9	40.0	4.0	2.9	**2.7**
	C-10	Concrete	23.6	22.3	80.6	61.3	22.9	10.8	**10.8**
	G-01	Gasket	(6.5)	(0.8)	0.9	0.8	2.6	2.4	**0.8**
	G-02	Gasket	(6.3)	(0.9)	1.4	2.5	1.7	28.5	**0.9**
	G-03	Gasket	(6.7)	1.4	10.9	10.3	0.9	3.6	**0.9**
	G-04	Gasket	(6.8)	4.7	975.3	143.8	8.1	1.8	**1.8**
	G-05	Gasket	129.4	560.0	181.3	141.8	1667.2	2.5	**2.5**
	G-06	Gasket	(5.7	(0.8)	17.6	6.7	9.8	0.9	**0.8**
	G-07	Gasket	(6.5)	(0.9)	7.9	11.3	11.8	1.9	**0.9**
	G-08	Gasket	83.7	232.6	78.0	57.0	674.9	5.3	**5.3**
	G-09	Gasket	(6.2)	1.0	32.7	58.1	10.3	1.4	**1.0**
	G-10	Gasket	(6.0)	1.0	31.7	55.6	10.6	1.4	**1.0**
	G-11	Gasket	(6.2)	1.1	37.0	59.1	10.8	1.5	**1.1**
	G-12	Gasket	91.9	4562.1	60.1	49.7	1627.0	37.8	**37.8**
	G-13	Gasket	(5.5	1.8	50.5	61.7	1.3	2.4	**1.3**
	G-14	Gasket	17.4	3.5	74.0	112.5	33.8	7.4	**3.5**
	G-15	Gasket	(6.4)	1.7	55.2	48.5	50.8	3.0	**1.7**
	G-16	Gasket	27.5	53.7	18.8	23.5	39.8	31.2	**18.8**
	G-17	Gasket	43.8	84.8	29.3	35.2	65.1	50.6	**29.3**
	G-18	Gasket	57.4	97.8	37.6	42.3	84.3	53.9	**37.6**
	G-19	Gasket	59.1	99.8	40.4	45.6	93.9	56.0	**40.4**
	G-20	Gasket	64.7	109.0	36.9	42.9	85.3	53.1	**36.9**
	G-21	Gasket	(6.7)	11.2	2.3	2.8	8.6	2.0	**2.0**
	G-22	Gasket	61.1	63.3	672.2	155.2	49.2	47.7	**47.7**
	G-23	Gasket	36.4	71.9	24.1	29.2	50.4	23.8	**23.8**
	G-24	Gasket	53.4	88.8	35.1	40.6	81.8	50.2	**35.1**
	G-25	Gasket	53.6	93.7	36.2	38.1	77.1	50.2	**36.2**
	V-01	Vinyl floor	(6.7)	3.4	0.6	2.5	(0.4)	1.1	**0.4**
	V-02	Vinyl floor	(6.8)	(0.9)	1.0	11.9	(0.8)	0.3	**0.3**
	V-03	Vinyl floor	(6.8)	(0.9)	1.0	3.7	(0.5)	1.9	**0.5**
	V-04	Vinyl floor	(6.8)	(0.9)	0.9	12.8	(1.0)	0.4	**0.4**
	V-05	Vinyl floor	(6.1)	(0.8)	9.9	48.6	(0.4)	20.6	**0.4**
	V-06	Vinyl floor	(6.2)	(0.9)	1.1	6.2	(0.6)	0.4	**0.4**
	V-07	Vinyl floor	27.1	39.7	38.4	17.2	49.0	19.2	**17.2**
	V-08	Vinyl floor	24.3	34.8	48.2	22.0	38.8	18.0	**18.0**
	V-09	Vinyl floor	116.6	149.5	138.8	101.4	138.9	41.8	**41.8**
	V-10	Vinyl floor	27.7	23.7	79.3	58.6	34.5	13.1	**13.1**
	V-11	Vinyl floor	19.4	28.2	31.9	34.4	39.2	12.0	**12.0**
	V-12	Vinyl floor	(5.7)	(0.8)	11.8	12.2	2.9	0.2	**0.2**
	V-13	Vinyl floor	(6.6)	(0.9)	24.1	5.1	122.7	1.2	**0.9**
	V-14	Vinyl floor	27.0	37.4	40.8	15.9	157.1	20.7	**15.9**
	V-15	Vinyl floor	11.0	18.3	76.0	26.7	36.9	11.0	**11.0**
CONTROL SET	C-11	Concrete	17.7	16.2	89.6	62.3	17.8	10.5	**10.5**
	C-12	Concrete	82.5	143.6	83.3	77.4	113.9	84.6	**77.4**
	C-13	Concrete	18.8	17.3	94.8	63.5	27.0	10.3	**10.3**
	C-14	Concrete	7.0	3.3	33.9	47.0	8.1	2.7	**2.7**
	C-15	Concrete	7.7	3.7	38.1	51.4	10.0	3.0	**3.0**
	G-26	Gasket	75.8	138.1	82.4	57.1	101.4	75.6	**57.1**
	V-16	Vinyl floor	1.1	0.4	4.4	1.2	8.3	0.8	**0.4**
	V-17	Vinyl floor	86.5	96.4	145.3	216.9	159.1	48.0	**48.0**
	V-18	Vinyl floor	25.0	32.6	37.1	25.0	53.2	21.4	**21.4**
	V-19	Vinyl floor	25.3	31.3	29.3	21.5	130.5	18.8	**18.8**
	V-20	Vinyl floor	1.4	0.5	3.3	1.5	1.2	0.5	**0.5**
	V-21	Vinyl floor	22.7	29.1	36.6	18.4	47.7	19.2	**18.4**
	V-22	Vinyl floor	13.4	17.4	30.7	33.2	15.1	4.4	**4.4**

Funding

This work was supported by the Italian Ministry of Health [Decreto dirigenziale del 27 dicembre 2017 e registrato dall'Ufficio Centrale di Bilancio il 24 gennaio 2018 al visto n. 460 - capitolo 4145 REACH].

REFERENCES

1. A kind of low temperature resistant modified EVA hot-melt adhesive of high viscosity and preparation method thereof. Inventor. Pan Minghua. China patent. 2017.
2. Some inorganic and organometallic compounds. IARC Monogr Eval Carcinog Risk Chem Man, 2 1973: 1-181.
3. Annex me of two Directive 76/769/EEC update. 1999; 99572.
4. World of Work Magazine. Asbestos in the workplace: a difficult legacy. 2004.
5. Survey, US Geological. 2017 Minerals Yearbook ASBESTOS [ADVANCE RELEASE]. 2020.
6. Gualtieri AF. Naturally Occurring Asbestos: A Global Health Concern? State of the Art and Open Issues. Environmental & Engineering Geoscience. 2020; 26: 3-8.
7. Schreier H. Asbestos in the natural environment. Earth and planetary sciences. 1989; 37: 159.
8. McCrone WC. Detection and identification of asbestos by microscopical dispersion staining. Environ Health Perspect. 1974; 9: 57-62.
9. Langer AM, Mackler AD, Pooley FD. Electron microscopical investigation of asbestos fibers. Environ Health Perspect. 1974; 9: 63-80.
10. Dollberg DD, Abell MT, Lange BA. Occupational Health Analytical Chemistry - Quantitation Using X-Ray Powder Diffraction. 1980; 43-65.
11. Luoma GA, Yee LK, Rowlond R. Determination of microgram amount of asbestos. Anal. Chem. 1982; 54: 2140-2142.
12. Perkins RL, Harvey BW. Method for The Determination of Asbestos in Bulk Building Ma Trials. U.S. Environmental Protection Agency. 1993.
13. Ingenieure VD. Determination of asbestos in technical products - Infrared Spectroscopy Method. VDI 3866- RICHTLINIEN. 2001; 19.
14. Accardo G, Cioffi R, Colangelo F, Angelo RD, De Stefano L, Paglietti F. Diffuse Reflectance Infrared Fourier Transform Spectroscopy for the Determination of Asbestos Species in Bulk Building Materials. Materials (Basel). 2014; 7: 457-470.
15. Gualtieri A, Artioli G. Quantitative determination of chrysotile asbestos in bulk materials by combined Rietveld and RIR methods. Powder Diffraction. 1995; 10: 269-277.
16. Foresti E, Gazzano M, Gualtieri AF, Lesci IG, Lunelli B, Pecchini G, et al. Determination of low levels of free fibres of chrysotile in contaminated soils by X-ray diffraction and FTIR spectroscopy. Anal Bioanal Chem. 2003; 376: 653-658.
17. European Regulation for the Registration, Evaluation, Authorisation and Restriction of Chemicals. Europ. Comm. 2006.
18. Malinconico S, Paglietti F, Serranti S, Bonifazi S, Lonigro I. Asbestos in soil and water: A review of analytical techniques and methods. J Hazard Mater. 2022; 436: 129083.
19. Pacella A, Fantauzzi M, Turci F, Cremisini C, Montereali MR, Nardi E, et al. Dissolution reaction and surface iron speciation of UICC crocidolite in buffered solution at pH 7.4: A combined ICP-OES, XPS and TEM investigation. Geochimica et Cosmochimica Acta. 2014; 127: 221-232.
20. Bloise A, Barca D, Gualtieri AF, Pollastri S, Belluso E. Trace elements in hazardous mineral fibers. Environ Pollut. 2016; 216: 314-323.
21. Gualtieri AF, Pollastri S, Gandolfi NB, Gualtieri ML. In vitro acellular dissolution of mineral fibres: A comparative study. Sci Rep. 2018; 8: 7071.
22. Thom JGM, Dipple GM, Power IM, Harrison EL. Chrysotile dissolution rates: Implications for carbon sequestration. Applied Geochemistry. 2013; 35: 244-254.
23. Morgan A. Acid Leaching Studies of Chrysotile asbestos from mines in the coalinga region of California and from Quebec and British Columbia. Ann Occup Hyg. 1997; 41: 249-268.
24. Bowes DR, Farrow CM. Major and Trace Element Compositions of the UICC Standard Asbestos Samples. Am J Ind Med. 1997; 32: 592–594.
25. Foresti E, Fornero E, Lesci IG, Rinaudo C, Zuccheri T, Roveri N. Asbestos health hazard: A spectroscopic study of synthetic geoinspired Fe-doped chrysotile. Journal of Hazardous Materials. 2009; 167: 1070-1079.
26. Pollastri S, D'Acapito F, Trapananti A, Colantoni I, Andreozzi GB, Gualtieri AF. The chemical environment of iron in mineral fibers. A combined X-ray absorption and Mossbauer spectroscopic study. J Hazard Mater. 2015; 298: 282-293.
27. Zeng B, Zang L, Li W, Li H, Wang H, Zhang M, et al. Quantitative analysis of asbestos in drinking water and its migration in mice using fourier-transform infrared spectroscopy and inductively coupled plasma optical emission spectrometry. Anal Chim Acta. 2019; 1058: 29-38.
28. Smith JG, HansonMerrill M. United States Brevetto US4260534A. 1979.
29. Nakao, Sadao. United States Brevetto 5443887A. 1992.
30. Dunuweera SP, Rajapakse RMG. Cement Types, Composition, Uses and Advantages of Nanocement, Environmental Impact on Cement Production, and Possible Solutions. Advances in Materials Science and Engineering. 2018: 1-11.
31. Witek J, Psiuk B, Naziemiec Z, Kusiorowski R. Obtaining an Artificial Aggregate from Cement-Asbestos Waste by the Melting Technique in an Arc-Resistance Furnace. Fibers. 2019; 7: 10.
32. Olivieri P, Malegori C, Mustorgi E, Casale M. Qualitative pattern recognition in chemistry: Theoretical background and practical guidelines. Microchemical Journal. 2021; 162: 105725.
33. Bonifazi G, Capobianco G, Serranti S. Asbestos containing materials detection and classification by the use of hyperspectral imaging. J Hazard Mater.2018; 344: 981-993.
34. Cossio R, Fraterrigo-Garofalo S, Avataneo C, Compagnoni R, Turci F, Zanella A, et al. Innovative unattended SEM-EDS analysis for asbestos fiber quantification. Talanta. 2018; 190: 158-166.
35. Olori A, Di-Pietro P, Campopiano A. Preparation of ultrapure KBr pellet, quantitative analysis. International Journal of Science Academic Research. 2021: 1015-1020.
36. Virta RL. Asbestos: Geology, Mineralogy, Mining, and Uses . Reston, VA: U.S. Department of Interior U.S. Geological Survey. 2002; 149.
37. Morgan A, Lally AE, Holmes A. Some observations on the distribution of trace metals in chrysotile asbestos. Ann occup Hyg. 1973; 16: 231-240.

38. O'hanley DS, Dyar MD. The composition of Chrysotile and its relationship with Lizardite. Canadian Mineralogist. 1998; 36: 727-739.

39. Bloise A, Ricchiuti C, Punturo R, Pereira D. Potentially toxic elements (PTEs) associated with asbestos chrysotile, tremolite and actionolite in the Calabria region (Italy). Chemical Geology. 2020; 30: 119896.

40. Conover W J. Practical nonparametric statistics. john wiley & sons. 1999.

41. Hartwig FP, Smith GD, Schmidt AF, Sterne JAC, Higgins JPT, Bowden J. The median and the mode as robust meta-analysis estimators in the presence of small-study effects and outliers. Res synth methods. 2020; 11: 397-412.

42. Manikandan S. Measures of central tendency: Median and mode. J Pharmacol Pharmacother. 2011; 2: 214-215.

43. Burdick RK, Sidor L, LeBlond DJ, Pfahler LB, Quiroz J, Vukovinsky K, et al. Statistical applications for chemistry, manufacturing and controls (CMC) in the pharmaceutical industry. Cham, Switzerland: Springer. 2017.

44. MacDougall D, Crummett WB. ACS. Guidelines for data acquisition and dada quality evaluation in Environmental Chemistry. Anal. Chem. 1980; 52: 2242-2249.

45. Ristic M, Czakò-Nagy I, Music S, Vértes A. Spectroscopic characterization of chrysotile asbestos from different regions. Journal of Molecular Structure. 2011; 993: 120-126.

46. Suquet H. Effects of dry grinding and leaching on the crystal structure of chrysotile. Clays and Clay Minerals. 1989; 37: 439-445.